

1 **Daily and intraseasonal relationships between lightning and NO₂ over the Maritime**

2 **Continent**

3 **(Supplementary material)**

4
5 Katrina S. Virts¹, Joel A. Thornton¹, John M. Wallace¹, Michael L. Hutchins²,
6 Robert H. Holzworth², and Abram R. Jacobson²

7
8 ¹Department of Atmospheric Sciences, University of Washington, Seattle, WA

9 ²Department of Earth and Space Sciences, University of Washington, Seattle, WA

10

10 **1. Statistical significance of correlations**

11 We elected to analyze GOME-2 NO₂ retrievals rather than SCIAMACHY retrievals in
12 hopes that the larger sample size provided by GOME-2's larger footprint would more than
13 compensate for the larger r.m.s. error of the GOME-2 retrievals. Using 3.5 years of daily
14 GOME-2 observations in 1281 1° × 1° grid boxes extending over the domain of the analysis
15 provides over 10⁶ observations. The effective number of temporal degrees of freedom of the
16 NO₂ observations for a given grid point, calculated using the formula of *Leith* [1973], is ≥ 650 .
17 In order to determine the statistical significance of composite correlation coefficients similar to
18 the composite regression coefficients in Fig. 2, it is also necessary to consider the spatial
19 dependence of the reference grid boxes. Using the eigenvalue method described by *Bretherton*
20 *et al.* [1999], the effective number of spatial degrees of freedom of the 100 reference grid boxes
21 used to construct Fig. 2 is ≥ 50 . Thus, the total effective number of degrees of freedom for
22 composite correlation coefficients between daily NO₂ concentrations and lightning flashes in the
23 1° × 1° grid boxes that were used to construct the regression maps in Fig. 2 is ≥ 30000 . Based
24 on the Student's *t* test, and assuming a two-sided distribution, this implies that composite
25 correlation coefficients of 0.02 are significant at the 99% level. The observed composite
26 correlations are on the order of 0.05 to 0.07. The high level of significance of the correlations is
27 evidenced by the smoothness of the patterns.

28

29 **2. Further specifics on the performance of WWLLN**

30 Daily WWLLN lightning observations summed over the Indonesian domain (10°S to
31 10°N; 90°E to 150°E) for the period of overlap with GOME-2 are shown in Fig. S1. The number
32 of detected lightning strokes has increased as more stations have been added to the network (e.g.,

33 the average detection efficiency for all lightning strokes in the United States has increased from
34 around 3% in 2005 to 11% in 2010 [*Jacobson et al.*, 2006; *Abarca et al.*, 2010]). *Rodger et al.*
35 [2009] compared lightning stroke observations from WWLLN and the New Zealand Lightning
36 Detection Network (NZLDN) from 2007 and found that WWLLN detected 10% or more of all
37 strokes over about 25 kA. Given the reasonably close proximity of New Zealand to our study
38 area, it is reasonable to take 10% as a first-order estimate of WWLLN's detection efficiency over
39 Indonesia during the period of overlap with GOME-2. Patterns very similar to those shown in
40 Figs. 1, 4, and S5 are obtained when the analysis is performed on lightning data restricted to the
41 period of overlap with GOME-2.

42 WWLLN's stroke detection efficiency has been compared in detail to simultaneous
43 observations by the far more sensitive Los Alamos Sferic Array [*Smith et al.*, 2002]. The
44 WWLLN detection efficiency was found in this manner to depend primarily on stroke current
45 amplitude, and not directly on stroke type [*Jacobson et al.*, 2006]. Thus, although not a "total
46 lightning" detection system, WWLLN is biased toward high current alone, and has no overt
47 selection for ground strokes over cloud strokes. To that extent, WWLLN might be expected to
48 serve as a reasonable interim proxy for lightning NO_x production, at least for the period before
49 total-lightning monitors are operational. WWLLN data do not provide any indication of stroke
50 altitude.

51 The median global very low frequency (VLF) stroke power measured by WWLLN is $3 \times$
52 10^6 W, more than three orders of magnitude smaller than that indicated by previous
53 measurements, which have shown the power radiated by strokes to be near 10^{10} W [*Krider and*
54 *Guo*, 1983]. However, this apparent discrepancy is due to the difference in methodology.
55 Previous measurements were of broad band peak power taken in the near field (within 100 km of

56 the lightning stroke), whereas WWLLN measures the r.m.s. power in the 6-18 kHz band in the
57 far field. With these factors accounted for, the median power is comparable to the previously
58 reported value of 10^{10} W [Kridner and Guo, 1983].

59

60 3. Sensitivity tests on daily lightning/NO₂ relationship and NO₂/stroke estimate

61 Figure 2 in *Virts et al.* [2011] shows the results of a composite lag regression analysis of
62 daily lightning frequency and tropospheric NO₂ column density fields over Indonesia (see text
63 for details). The composite analysis was based on the reference boxes indicated in Fig. S2. To
64 test the robustness of these results, we have conducted a series of sensitivity studies, varying the
65 following aspects of the analysis (note that for each estimate of NO₂ production, a WWLLN
66 detection efficiency of 10% was assumed).

- 67 • **Cloud fraction threshold** The results shown in *Virts et al.* [2011] were obtained by
68 analyzing only tropospheric NO₂ retrievals classified as “meaningful” by the GOME-2
69 quality control algorithms [Boersma et al., 2004]. To test the impact of cloudy
70 observations, the composite lag regression analyses were repeated with NO₂ time series
71 that incorporated only observations for which the FRESCO cloud fraction [Koelemeijer
72 et al., 2011] was below 0.1 (Fig. S3, top row).
- 73 • **Sample size** Although it is clearly desirable to choose reference boxes for which there is
74 sufficient lightning to provide a day-to-day signal, our selection of the 100 grid boxes
75 with the highest annual-mean lightning frequencies is somewhat arbitrary. Lag
76 regression analyses performed on reference boxes with lightning frequencies in the top 50
77 and 500 are shown in the second and third rows of Fig. S3.

78 • **Location of reference boxes** The reference boxes used in the analysis in Fig. 2 are
79 located over land or along the coasts of the Indonesian islands (Fig. S2). To test whether
80 our results are sensitive to possible changes in the NO₂ plume from surface sources along
81 the islands, the lag regression analysis was repeated using a set of reference boxes located
82 over water or over less polluted land areas, as indicated in Fig. S4. The associated
83 composite NO₂ regression patterns are shown in the bottom row of Fig. S3.

84 Comparison of Fig. S3 and Fig. 2 in the text shows that the spatial pattern and temporal
85 evolution of the NO₂ field are robust with respect to variations in the analysis protocol. The
86 production efficiencies estimated on the basis of these various protocols were used to obtain the
87 estimated range of 1.7 to 2.5×10^{25} NO₂ molecules per stroke put forth in *Virts et al.* [2011].

88

89 **4. MJO correlation maps**

90 Figure S5 shows maps of correlation coefficients between the MJO index and clouds,
91 lightning, and NO₂, analogous to the maps of regression coefficients shown in Fig. 4 in the text.
92 It is evident that the MJO signal in lightning and NO₂ over the eastern Indian Ocean is strongest
93 just to the west of Sumatra, within the region in which mesoscale circulations driven by land/sea
94 contrasts and terrain play an important role in triggering convection. In the correlation maps a
95 weak enhancement of lightning is also apparent over new Guinea in phases 1 and 2, which is
96 mirrored in the NO₂ regression pattern.

97

98 **5. Alternative explanations for NO₂ patterns**

99 In this section we examine three factors that can influence tropospheric NO₂ column
100 retrievals and discuss whether they could produce NO₂ patterns similar to those shown in *Virts et*
101 *al.* [2011].

- 102 • **Tropopause height variations.** Tropospheric NO₂ vertical column densities are
103 obtained from total atmospheric slant column densities by subtracting an assumed
104 stratospheric NO₂ column and dividing by a tropospheric air mass factor [*Boersma et al.*,
105 2004]. The MJO modulates cold-point tropopause height; however, these variations are
106 on the planetary scale [e.g., *Zhang, 2005; Virts and Wallace, 2010*] and thus cannot
107 explain the more localized NO₂ patterns in Figs. 4 and S5.
- 108 • **Transport of non-lightning NO₂.** NO₂ produced by surface sources can be transported
109 by convection to the upper troposphere, where its lifetime is longer and where it is more
110 readily visible to the satellite. Winds can also transport NO₂ horizontally, as seen in Fig.
111 2 in the text. We have demonstrated that the plume of enhanced NO₂ associated with a
112 lightning maximum is present regardless of whether we use reference boxes over the
113 ocean or over less polluted land areas (Fig. S4). In addition, the MJO NO₂ signature in
114 Figs. 4 and S5 is strongest to the west of Sumatra, where the influence of surface sources
115 of NO₂ is much lower (e.g., Fig. 1).
- 116 • **Cloud contamination.** The dissimilarities in the cloud and NO₂ patterns in Figs. 1 and 4,
117 combined with the fact that the NO₂ patterns in Figs. 2 and 4 do not change when only
118 NO₂ retrievals with cloud fractions below 0.1 are included in the analysis (see, e.g., Fig.
119 S3), indicate that cloud contamination is not a significant issue for these analyses, though
120 it may need to be taken into account in quantifying the lightning NO_x source.

121 Thus, while each of these factors influences GOME-2's tropospheric NO₂ retrievals, none
122 can account for the NO₂ patterns associated with lightning shown in the text. Other factors that
123 impact tropospheric NO₂ retrievals are discussed in *Boersma et al.* [2004].

124

125 **References**

126 Abarca, S. F., K. L. Corbosiero, and T. J. Galarneau Jr. (2010), An evaluation of the Worldwide
127 Lightning Location Network (WWLLN) using the National Lightning Detection Network
128 (NLDN) as ground truth, *J. Geophys. Res.*, *115*, D18206, doi:10.1029/2009JD013411.

129 Beirle, S., H. Huntrieser, and T. Wagner (2010), Direct satellite observation of lightning-
130 produced NO_x, *Atmos. Chem. Phys.*, *10*, 10965-10986.

131 Boersma, K. F., H. J. Eskes, and E. J. Brinksma (2004), Error analysis for tropospheric NO₂
132 retrieval from space, *J. Geophys. Res.*, *109*, D04311, doi:10.1029/2003JD003962.

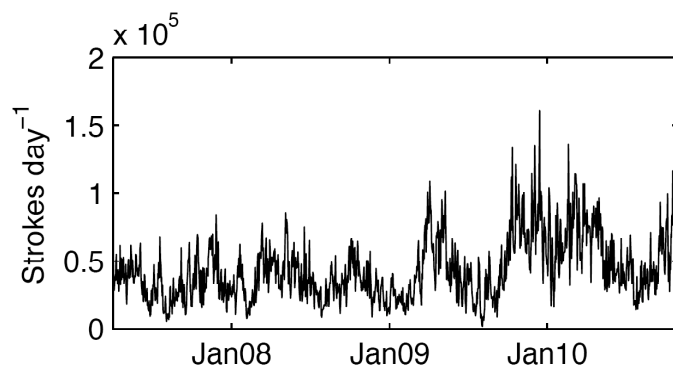
133 Bretherton, C. S., M. Widmann, V. P. Dymnikov, J. M. Wallace, and I. Bladé (1999), The
134 effective number of spatial degrees of freedom of a time-varying field, *J. Climate*, *12*,
135 1990-2009.

136 Jacobson, A. R., R. H. Holzworth, J. Harlin, R. L. Dowden, and E. H. Lay (2006), Performance
137 assessment of the World Wide Lightning Location Network (WWLLN), using the Los
138 Alamos Sferic Array (LASA) as ground-truth, *J. Atmos. Ocean. Tech.*, *23*, 1082-1092.

139 Koelemeijer, R. B. A., P. Stammes, J. W. Hovenier, and J. F. de Haan (2001), A fast method for
140 retrieval of cloud parameters using oxygen A band measurements from the Global Ozone
141 Monitoring Experiment, *J. Geophys. Res.*, *106*, 3475-3490.

142 Krider, E. P., and C. Guo (1983), The peak electromagnetic power radiated by lightning return
143 strokes, *J. Geophys. Res.*, *88(C13)*, 8471-8474, doi:10.1029/JC088iC13p08471.

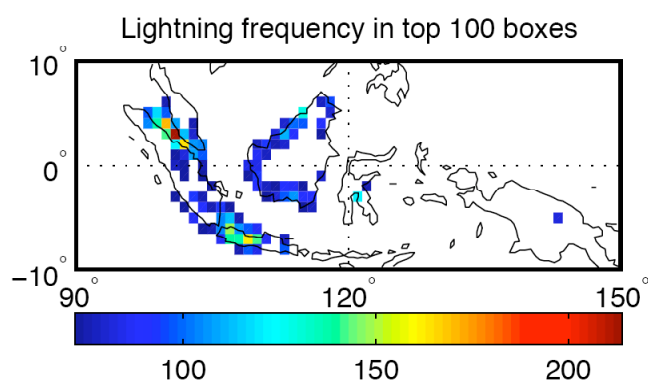
- 144 Leith, C. E. (1973), The standard error of time-averaged estimates of climatic means, *J. Appl.*
145 *Meteor.*, *12*, 1066-1069.
- 146 Rodger, C J, J B Brundell, R H Holzworth, and E H Lay (2009), Growing Detection Efficiency
147 of the World Wide Lightning Location Network, *Am. Inst. Phys. Conf. Proc.*, Coupling
148 of thunderstorms and lightning discharges to near-Earth space: Proceedings of the
149 Workshop, Corte (France), 23-27 June 2008, 1118, 15-20, DOI:10.1063/1.3137706.
- 150 Smith, D. A., K. B. Eack, J. Harlin, M. J. Heavner, A. R. Jacobson, R. S. Massey, X. M. Shao,
151 and K. C. Wiens (2002), The Los Alamos Sferic Array: A research tool for lightning
152 investigations, *J. Geophys. Res.*, *107(D13)*, doi:10.1029/2001JD000502.
- 153 Virts, K. S., J. A. Thornton, J. M. Wallace, M. L. Hutchins, R. H. Holzworth, and A. R. Jacobson
154 (2011), Daily, seasonal, and intraseasonal relationships between lightning and NO₂ over
155 the Maritime Continent, *Geophys. Res. Lett.*, ???.
- 156 Virts, K. S., and J. M. Wallace (2010), Annual, interannual, and intraseasonal variability of
157 tropical tropopause transition layer cirrus, *J. Atmos. Sci.*, *67*, 3097-3112.
- 158 Zhang, C., (2005), Madden-Julian Oscillation, *Rev. of Geophys.*, *43*, RG2003,
159 doi:10.1029/2004RG000158.
- 160



160 **Figure S1.** Time series of daily lightning strikes detected by WWLLN over Indonesia.

161

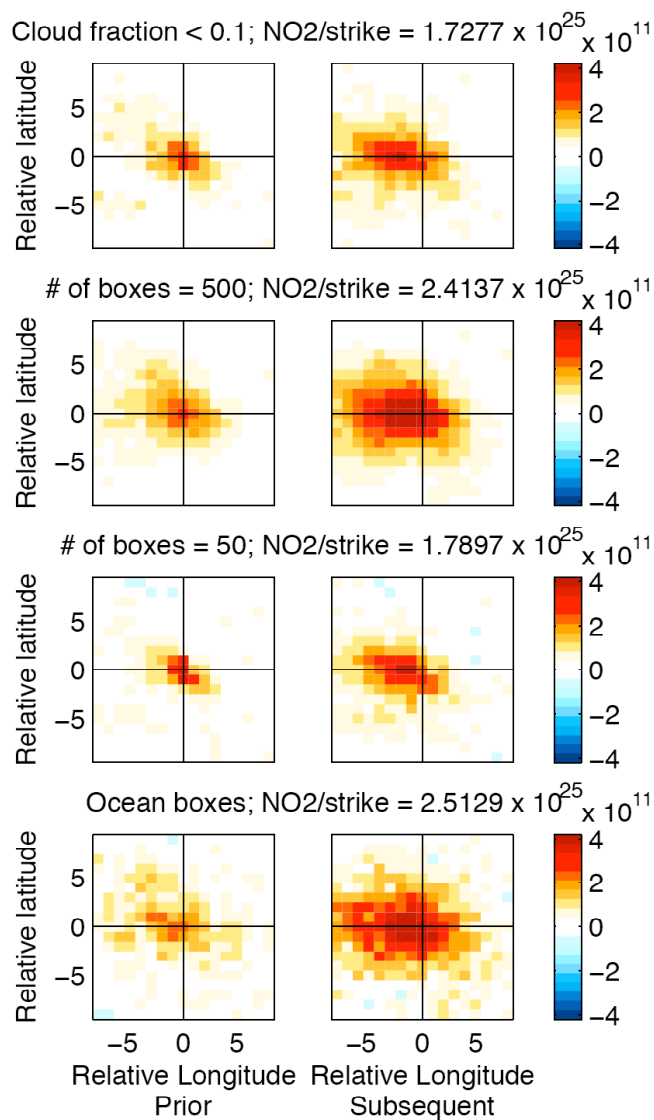
162



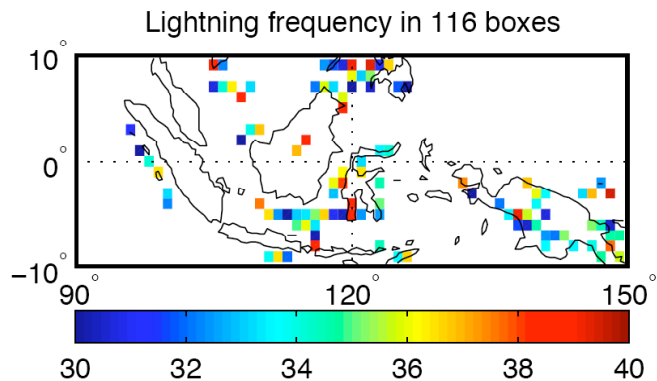
163 **Figure S2.** Map of 100 grid boxes with highest annual-mean lightning frequency. These
164 reference boxes were used to generate the composites in Fig. 2.

165

166

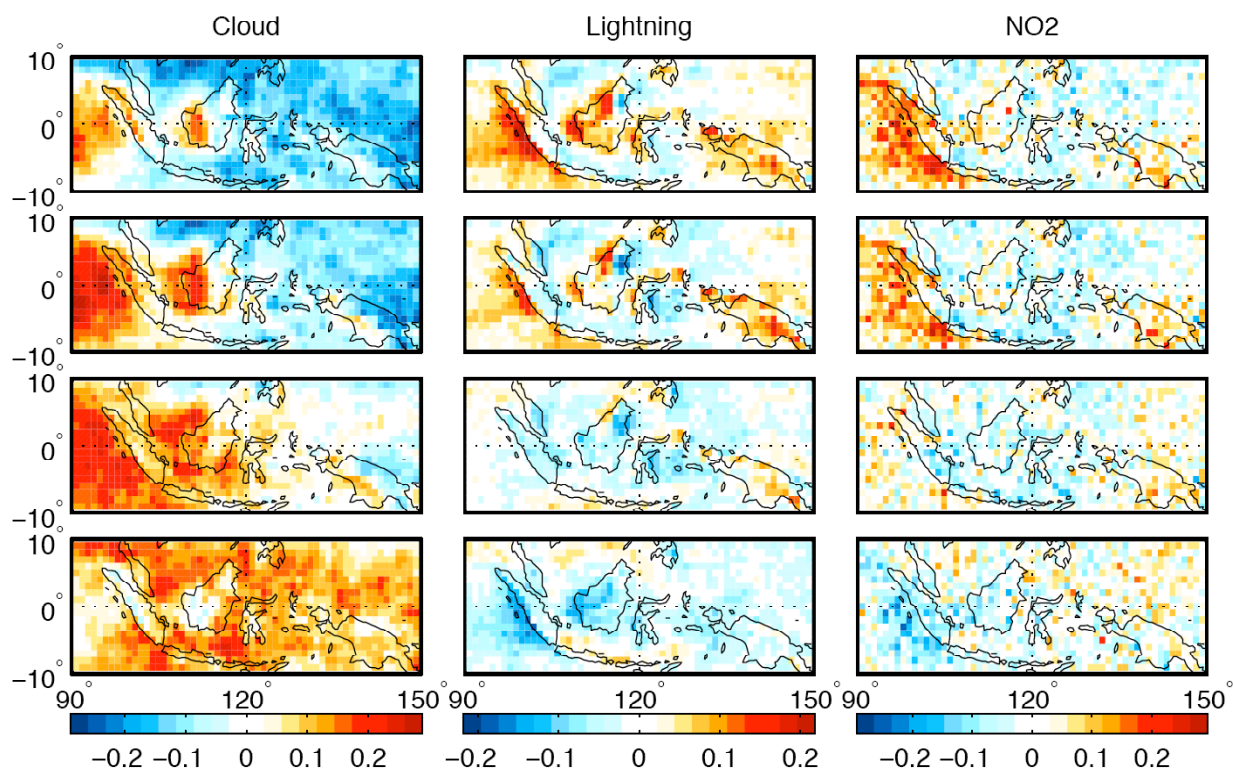


166 **Figure S3.** As in Fig. 2, but regressions were calculated using NO₂ time series based on only
 167 those observations with FRESCO cloud fractions less than 0.1 (top row), the indicated number of
 168 reference boxes (second and third rows), and the reference boxes shown in Fig. S4 (bottom row).



169 **Figure S4.** Annual-mean lightning frequency in selected grid boxes over water or less polluted
 170 land areas.

171
 172



173 **Figure S5.** As in Fig. 4, but cloud, lightning, and NO_2 are correlated with MJO indices.